UNIVERSITI TEKNOLOGI MARA

ISO 9001:2000 No Sijil :0500132

Globalising Knowledge and Information

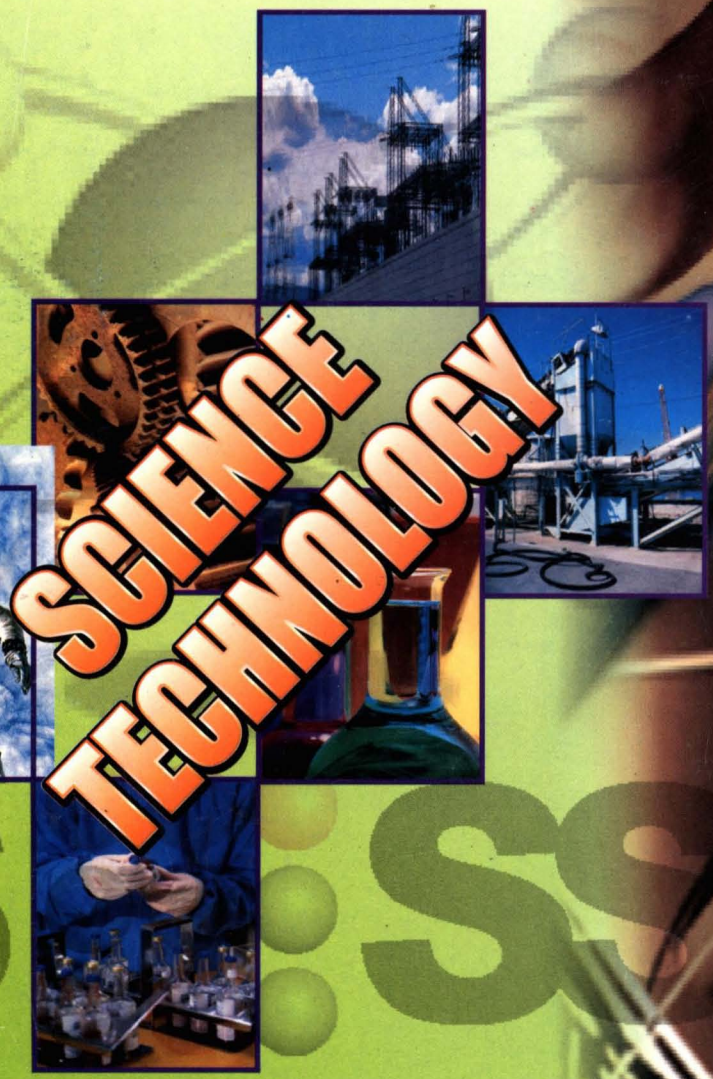

NATIONAL SEMINAR ON SCIENCE TECHNOLOGY & SOCIAL SCIENCES 2006

30-31 May 2006

Swiss Garden Resort & Spa

Kuantan, Pahang

A Computational Study of Brain Fluid Flow within the Human Ventricular System

A. Aroussi
B. Howden
M. Vloeberghs

ABSTRACT

A three dimensional (3D) model of the Human Ventricular System (HVS) is presented to investigate the flow of Cerebrospinal Fluid (CSF) within the human brain, using Computational Fluid Dynamics (CFD). The role of CSF is complex but can be split into two main areas: a) acting as a buffer between the brain and the skull, b) acting as a transport medium for compounds and nutrients. CSF can be modelled as a Newtonian Fluid and its flow through the HVS can be visualized using CFD. In this investigation a 3D geometric model of the HVS (Fig. 1) was constructed from MRI data. It is the only model of its type to date. The flow of CSF within the HVS is a complicated phenomenon due to the complex HVS geometry. Previous modelling has only looked at individual parts of the HVS rather than as a whole. Understanding the nature of CSF flow allows engineers and physicians to design medical techniques and drugs to treat various HVS complications, such as hydrocephalus resulting from a tumor in the HVS. During this investigation CSF flow rate was set as 500ml/day, to mimic real life conditions, and secreted into the model via three inlets, with a uniform velocity. The model also contained three outlets, modelled as pressure outlets. The flow pattern of the CSF was found to vary with location, with the fastest flow being found in the Cerebral Aqueduct; a maximum velocity of 10mm/s was observed in this area. CSF pressure also varied with geometry and a negative pressure gradient was observed in the z-direction. The highest pressure drop also occurred through the Cerebral Aqueduct. The results of the investigation show that CSF flow is laminar and that the velocity is fastest within the Cerebral Aqueduct. Also CSF flow velocity is substantially slower in the areas of the HVS that are furthest away from the inlets; in some areas flow is virtually stagnated.

Keywords : *Brain fluid flow, human ventricular system, computational fluid dynamics*

Introduction

The role of Cerebrospinal Fluid (CSF), its passage from secretion by the Choroids Plexus to absorption at the Pacchionian granulations, and its use for delivering medical drugs to areas of the body, have been the source of much debate within the medical community

Since the early discoveries by Cotungo, Magendie and Faivre (Greitz et al. 1992) which helped to establish the nature of CSF, much work has been carried out on the movement of CSF using various techniques, most recent those of radionuclide cisternography coupled MRI to view CSF flow (Greitz 1993). With advances in computer processors work has also been undertaken computationally using CFD to model CSF flow and understand its nature (Loth, Yardimci and Alperin 2001; Aroussi, Zainy and Vloeberghs 2000; Howden, Aroussi and Vloeberghs 2002; Jacobson et al. 1996, 1999).

The function of CSF is generally accepted as two fold: cushioning the brain from impact on the cranial vault (Loth, Yardimci and Alperin 2001). and transportation of biomechanical substances to and from the brain (Greitz et al. 1992). CSF is in direct communication with major areas of the brain and therefore, in theory, can be used as a transport medium, allowing the delivery of locally injected drugs to areas of the brain and Central Nervous System (CNS) where treatment is needed (Siegal and Zylber-Katz 2002). Examples of such cases include of non-communicating hydrocephalus, resulting from of a tumour in the cerebral aqueduct, which causes little or no CSF flow within the cerebral ventricles, creating a pressure build up that could be fatal if not treated (Howden, Aroussi and Vloeberghs 2002; Aroussi, Zainy and Vloeberghs 2000).

The general movement of CSF through the HVS has been thoroughly documented (Greitz et al. 1992; Greitz 1993; Siegal and Zylber-Katz 2002; Redzic and Segal 2004; Perez-Figares, Jimenez and Rodriguez 2001). The HVS consists of four cavities (ventricles): two large lateral ventricles, the third ventricle, which is connected to the lateral ventricles via two inlets (Foramina of Monro) and fourth ventricle, which is connected to the third via the cerebral aqueduct called the 'Aqueduct of Sylvius' (Greitz et al. 1992; Greitz 1993; Perez-Figares, Jimenez and Rodriguez 2001). A representation of the HVS is shown in Figure 1 (Marieb 2004).

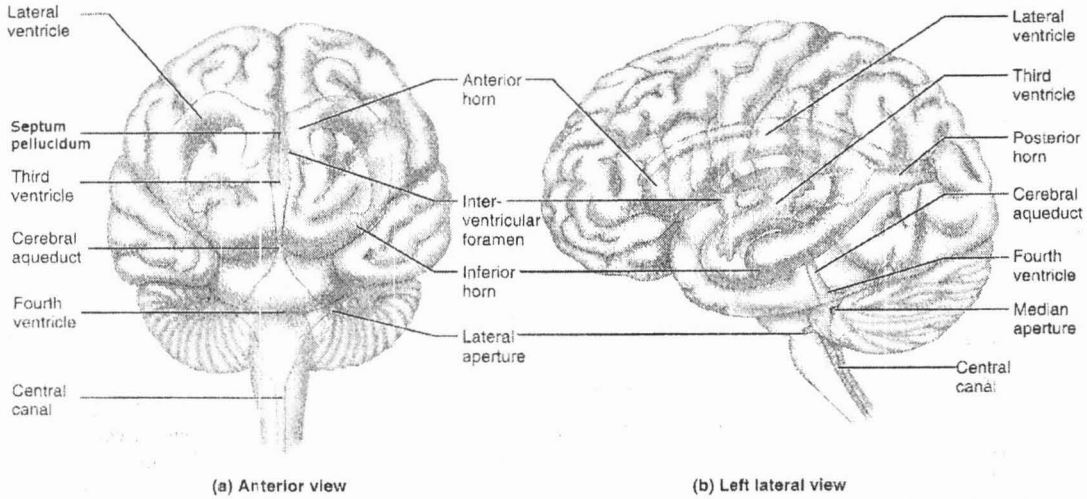

Fig. 1 : Illustration of the anatomy and location of the Human Ventricular System (Marieb 2004).

In previous years a lack of specific knowledge as to the exact fluid dynamics of CSF has hampered efforts to discern the validity of local cerebral drug delivery as a medical technique. With the onset of more accurate modelling techniques there has been a marked increase in amount of work being carried out on the dynamics of CSF particularly on the aqueduct region of the HVS (Zainy 2002; Aroussi, Zainy and Vloeberghs 2000; Jacobson et al. (1996, 1999); Fin and Grebe 2003). Jacobson et al. (1996, 1999) were the first to look at modelling any part of the HVS in detail. Their paper looked at various models of the aqueduct of Sylvius, comparing CSF flow through varying geometrical shapes for the aqueduct. The results of their investigation showed that for a daily CSF production of 579ml the pressure drop along the aqueduct was 1.1Pa. Further work by Jacobson et al. (1999) looked at a case of aqueduct stenosis and showed that for even mild cases the pressure needed to drive a flow rate of 579ml/day of CSF increased by 100 times. Work on modelling the aqueduct of Sylvius has also been carried out by Aroussi *et al.* (2000). By examining varying production rates of CSF it was found that the highest velocity through the aqueduct occurred in the neck area, i.e. at the top of the aqueduct. It was also seen that the area of highest velocity is also the area where the largest wall shear stress was observed. High wall shear is dangerous as it can lead to medical complications. Work by Zainy (2002) has further examined the three-dimensional flow of CSF through the cerebral aqueduct, showing that CSF flow is laminar in nature and that both maximum velocity within the aqueduct and wall shear stress increase with increasing production of CSF. Current work by Fin & Grebe has looked at pulsatile CSF flow within the aqueduct of Sylvius noting CSF velocities of up to 60 mms-1 (Fin and Grebe 2003).

In this paper we present an application of CFD to model the 3D flow of CSF inside the HVS, with a view to ascertaining the nature of CSF flow within this important compartment of the brain. The understanding of the 3D CSF flow will allow for a greater understanding of CSF production, movement and possible uses of CSF.

Methodology

Model Generation

A three dimensional (3D) model of the Human Ventricular System (HVS) has been produced computationally using Magnetic Resonance Imaging (MRI) data. MRI scans of a healthy volunteer were taken using T2 weighted Constructive Interference in Steady State (CISS). The MRI images were set at 1mm apart over the length of the body. Once successfully scanned the individual MRI images were transferred electronically to MRI conversion software called MIMICS (Materialise, Holland). MIMICS is an integrated 3D image processing and editing software that allows MRI data to be converted into other suitable data formats, for computational analysis. MIMICS uses threshold separation to capture various individual regions in an MRI slice and was used to identify the contrast between CSF and brain material. After thresholding, the full ventricular system was extracted as a Stereo Lithography file (STL).

Once in STL format the MRI data, now represented as a solid shelled model, was transferred to another software package called MAGICS (Materialise, Holland). MAGICS is a STL manipulation software and was used to correct the raw STL file, produced by MIMICS. MAGICS was used to generate accurate outlets and inlets to represent the true geometry of the ventricular system (Figure 1). In all the three exits at the base of the ventricular system and the

choroids plexii of the lateral and fourth ventricles were incorporated into the Ventricular Model. The choroids plexus of the third ventricle was not represented in the model, due to technical difficulties. An illustration of the mesh model, as produce by GAMBIT, is shown in Figure 2.

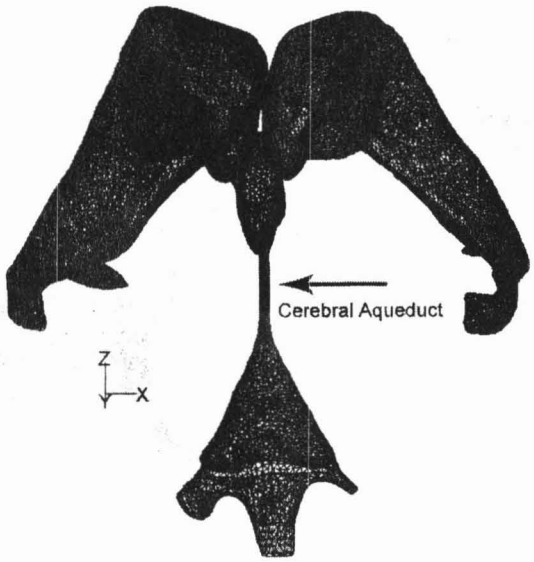

Fig. 2.: 3D model of the HVS produced in GAMBIT, using MRI data

Numerical methods

The STL model was exported to the CFD package GAMBIT, a meshing program, that allowed the STL file to be converted from a shell into a volume filled with tetrahedral cells, of 2mm edge length. The volume mesh is comparable to the numerical solution of the fluid flow. Using GAMBIT the boundaries were applied to the model with the three outlets modelled as pressure outlets and the Choroids Plexii modelled as velocity inlets.

The commercial CFD code FLUENT™, a fluid flow modelling software, was used to calculate the CSF flow dynamics within the ventricular model. FLUENT™, uses the the Finite Volume Method to analyze the flow dynamics of the CSF within the ventricular system by solving the Navier-Stokes equations that govern 3D flow in incompressible fluids, of which CSF can be modelled as Davson et al. (1987). The SIMPLE (Semi Implicit Method for Pressure-Linked Equations) algorithm was utilized during the solving of the case.

The model was set up as a rigid walled, steady state model, despite the known flexibility of the ventricles and the pulsatile nature of CSF. This setup allowed for analysis of the role of CSF production in isolation, before the incorporation of pulsatile movement at a later date.

The choroids plexii were set as constant velocity inlets to mimic the constant production of CSF taken to be 500ml per day (Davson, Welch and Segal 1987). The outlets at the foramina of Lushka and the foramen of Magendie were set as pressure outlets, to allow the examination of the pressure field within the HVS. The outlets were given a gauge pressure of Zero Pa, which was taken to allow for a pressure gradient to develop over the flow field. The operating pressure was 1 atmosphere. The effect of external hydrodynamic pressure was ignored since the ventricles are in a near neutral buoyant environment within the brain.

The internal surfaces of the ventricles were modelled as non-slip, with zero velocity on the walls. Although ventricular cilia are present within the lateral ventricles, a boundary condition to model the effect of these cilia accurately has not previously been considered to the knowledge of the authors and will require further development beyond the scope of this paper. Gravity was not incorporated into this model and therefore buoyancy has been ignored in the Navier-Stokes equations.

The fluid was modelled as CSF with a viscosity of 0.0008 Pa.s and density 1005 kgm^{-3} (Davson, Welch and Segal 1987). The flow of CSF was modelled as laminar as it is secreted at very low velocities (creep velocities) and therefore has a low Reynolds Number. Figure 2.1 shows the finalised version of the 3D HVS once it was successfully loaded into FLUENT™.

Results and Discussion

FLUENT™ is a very useful tool to analyse the flow of CSF as it provides a non-invasive and in-expensive method to gather hydrodynamic and parametric information about CSF movement. Of primary importance in the study was to ascertain the velocity characteristics of CSF throughout the flow field of the HVS. Understanding the velocity pattern of the CSF is essential if the goal of Intra-ventricular drug delivery is to be examined.

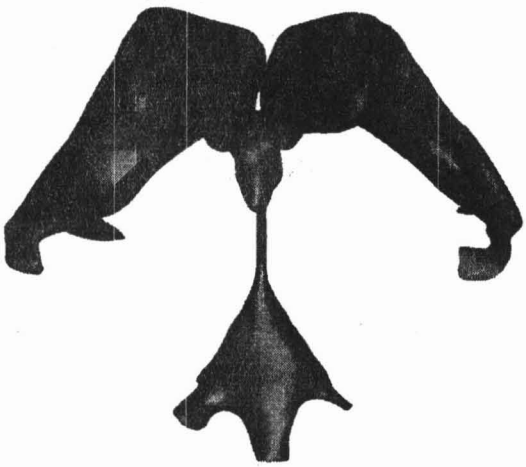

Fig. 2.1:- Front view of rendered 3D model of the HVS produced in FLUENT™

General findings

Figures 3.0 and 3.1 show the overall velocity vectors of the CSF (front and left views) within the HVS. As shown by figures 3.0 and 3.1 the highest CSF velocities occur within the cerebral aqueduct, however there are a number of regions within the HVS that have CSF flow velocities less than 10 nano ms^{-1}.

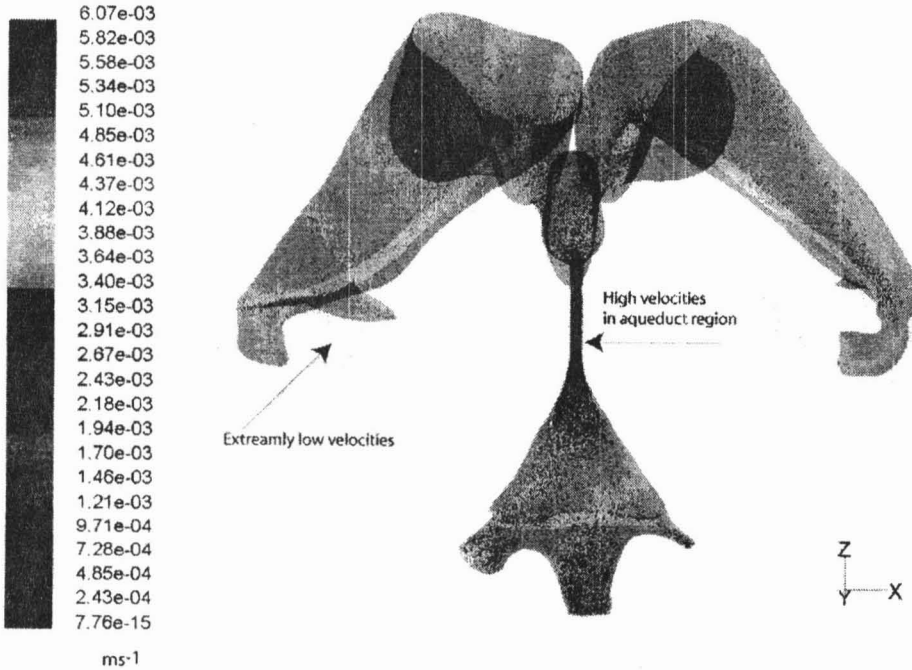

Fig. 3.0: Front view of the HVS showing the general CSF flow velocities; areas of highest and lowest CSF velocity are highlighted

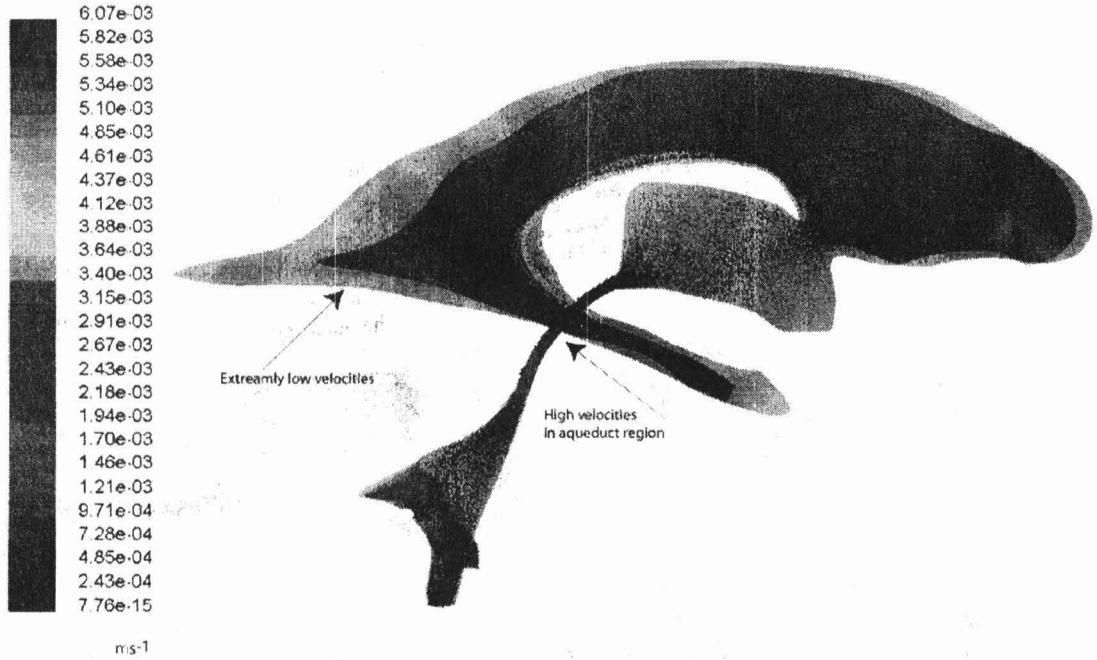

Fig. 3.1: Left view of the HVS showing the general CSF flow velocities; areas of highest and lowest CSF velocity are highlighted

As can also be seen from figure 3.0 and 3.1 is the general flow of the CSF from the inlets at the choroids plexii to the exits at the bottom of the HVS. Figure 3.2 shows the flow in more detail and also helps to explains the areas of extremely slow flow seen in figure 3.0 and 3.1

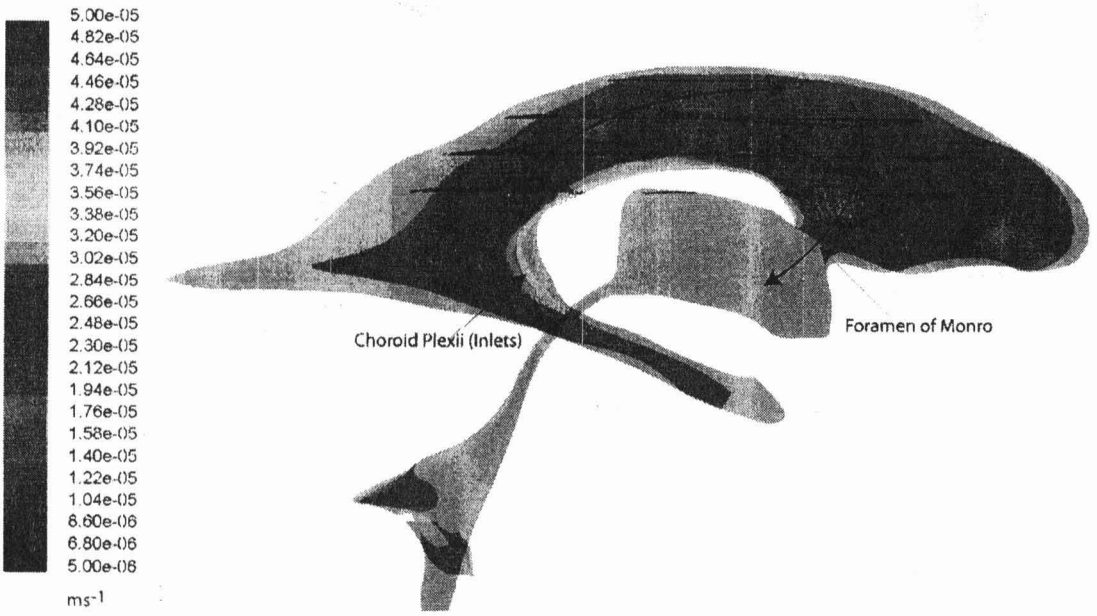

Fig. 3.2: Left view of the HVS showing the general CSF flow pattern; velocity vectors are projected onto planes taken in the z direction.

As shown in figure 3.2 the CSF flow rises from the inlets at the choroids plexii. The velocities of CSF are highest close to the inlets and slower at distances distal to the inlets. This helps to explain the areas of low CSF velocity seen in figures 3.0 and 3.1, as the majority of the fluid flows through the centre of the HVS towards the pressure outlets at the bottom of the HVS. Little CSF flow is directed towards the back of the HVS; hence CSF velocity is extremely low in the regions identified in 3.0 and 3.1.

As shown by figure 3.2 and also figure 3.3, CSF follows the path outlined by various authors (Zainy 2002; Greitz *et al.* 1992; Perez-Figares, Jimenez and Rodriguez 2001; Davson, Welch and Segal 1987), flowing from the inlets, through the foramen on Monro into the third ventricle. As seen in figures 3.2 and 3.3 the CSF velocity increases as it flows towards the Foramen of Monro and then increases again as it flows through the third ventricle, with the fastest CSF flow in the centre and slower flow near the outer regions of the third ventricle.

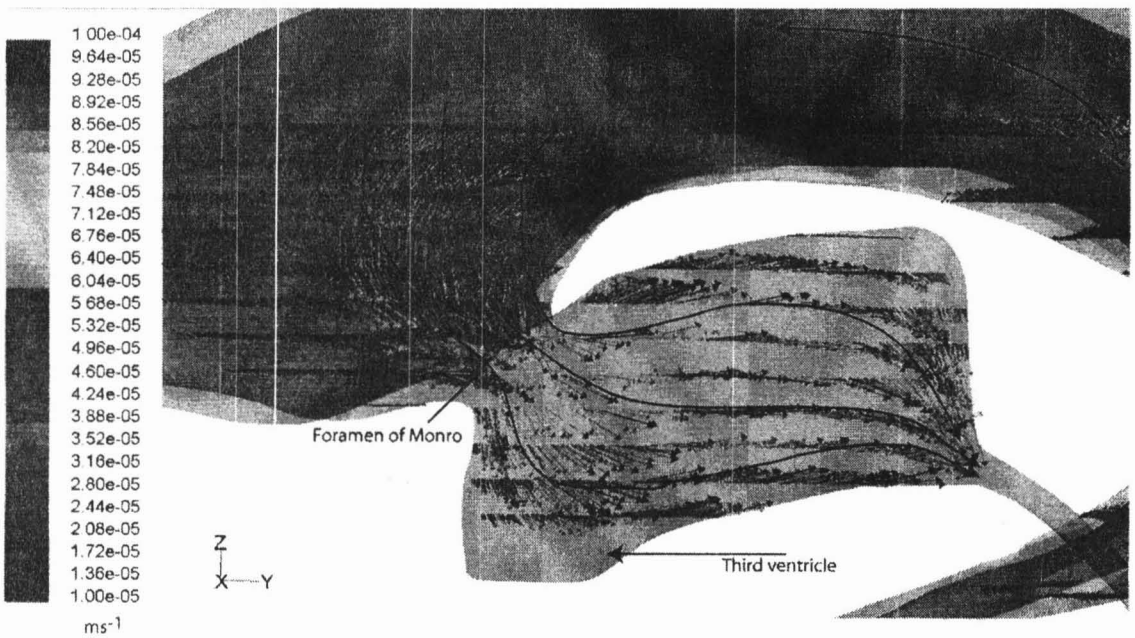

Fig. 3.3: Left isometric view of part of the HVS showing the general CSF flow pattern as it moves from the lateral ventricles, through the Foramen of Monro and in to the third ventricle; velocity vectors are projected onto planes taken in the z direction.

As the HVS was modelled as a closed system, without gravity, the pressure through the system will vary with CSF flow velocity, due to equation 1.0.

$$\rho g h + P_s + \frac{1}{2}\rho u^2 = P_c$$

1.0

Where ρgh is zero due to hydrodynamic pressure being ignored (see section 2.2), Ps is the static pressure on the ventricles, which is constant, and ½ρu2 is the dynamic pressure. Therefore as velocity, u, increases the dynamic pressure increases and therefore the overall pressure in the system will decrease at a larger rate; pressure decreases through system as the outlets were modelled as pressure outlets of Zero Pa. Figure 3.4 shows the pressure distribution through the HVS.

As can be seen in figure 3.4 the pressure varies through the HVS with the largest pressure drop occurring through the aqueduct, due to the higher dynamic pressure caused by larger CSF velocities in this part of the HVS. Section 3.2 highlights this region in more detail.

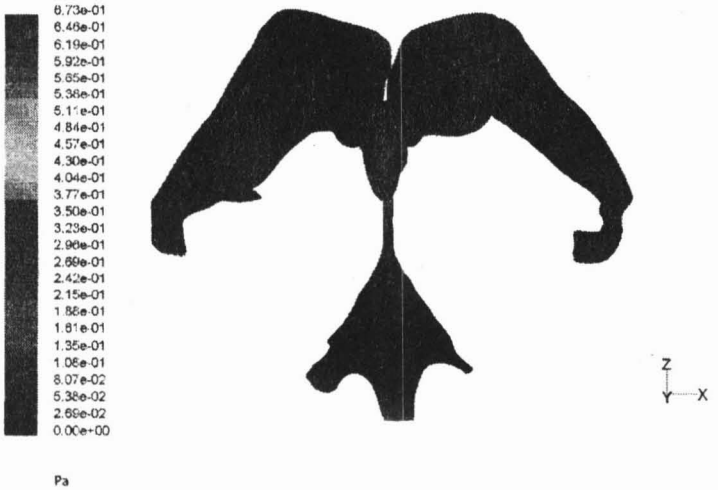

Fig. 3.4: Front view of the HVS showing the pressure distribution in the Z-direction, down through the system.

Aqueduct region

As referred to in section 3.1 the aqueduct region is by far the most active area within the HVS, seeing the highest velocities and also the largest pressure drop over the system. Figure 3.5 shows a detailed view of the CSF velocity vectors and velocity contours in this region, with figure 3.6 showing a graph of the CSF velocity down the aqueduct.

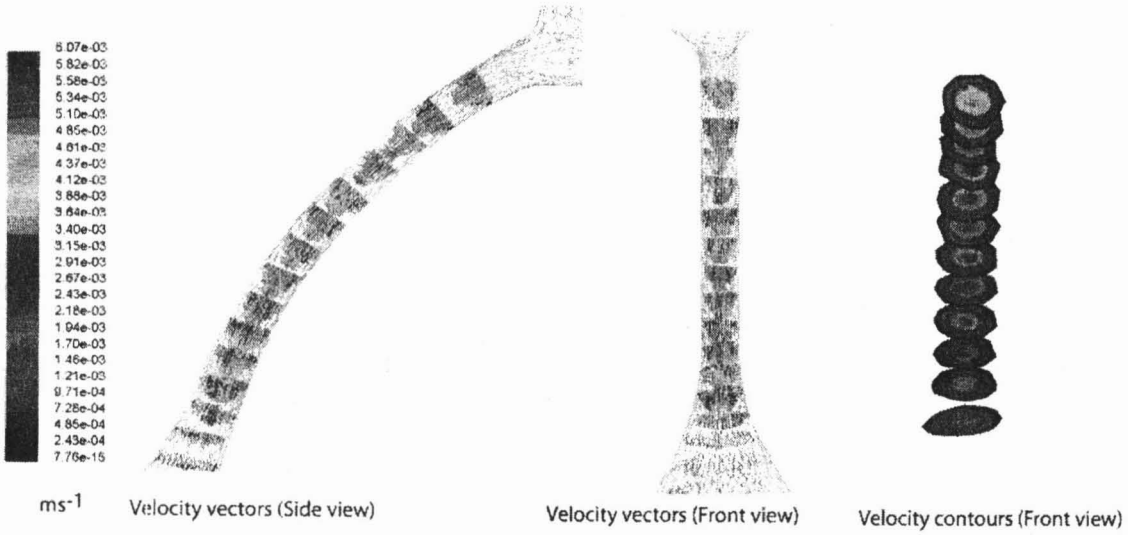

Fig. 3.5: Front and left views of the HVS showing the velocity distribution in the Z-direction, down through the aqueduct region.

As can be seen from figure 3.5 the highest CSF velocity within the aqueduct, and therefore the HVS, is in the region of 6.07mm/s and occurs at approximately 3mm down the aqueduct (figure 3.6), with the fastest CSF velocities generally occurring through the centre of the aqueduct. Figure 3.6 shows the CSF velocity profile through the aqueduct. It can be seen that after 13mm the CSF velocity slows down, as it enters the larger volume of the fourth ventricle. These findings are consistent with the work of various authors (Zainy 2002; Greitz et al. 1992; Howden, Aroussi and Vloeberghs 2002). Zainy (2002) modelled the cerebral aqueduct and found CSF velocities to be fastest in the top neck region, recording a maximum velocity in the region of 5.6mm/s. Greitz et al. (1992) have also found CSF velocities in the order of 5-10mm/s within the cerebral aqueduct.

Figure 3.7 shows the pressure drop down the aqueduct. As can be seen, the pressure drop over the aqueduct is 0.62 Pa, which is consistent with the findings of Jacobson *et al.* (1996), who showed that a pressure drop of 1.1 Pa was necessary to drive a flow of higher CSF production through the cerebral aqueduct. The findings are also consistent with those of Fin and Grebe (2003), who used a rigid walled cylinder to model the aqueduct and found a pressure of 1.02 Pa was required to force 42mm^3/s of CSF through the aqueduct.

Fig. 3.6: CSF velocity distribution in the Z-direction, down through the aqueduct region.

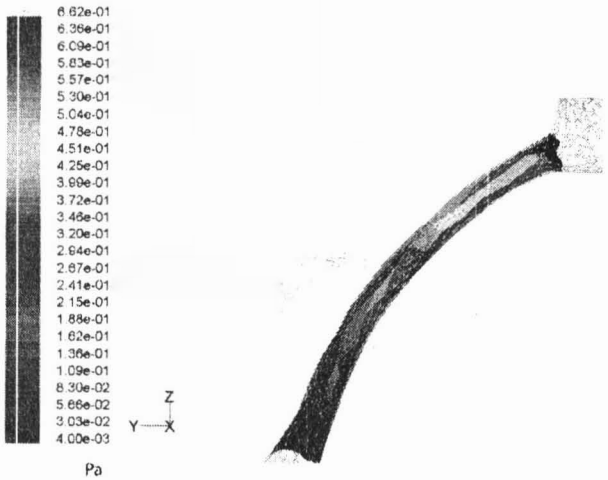

Fig. 3.7: CSF pressure distributions in the Z-direction, down through the aqueduct region.

Conclusion

The 3D model presented in this paper provides a detailed analysis of the flow dynamics within the human ventricular system. The results generated show that CSF velocity can reach up to 6 mm/s within the cerebral aqueduct by daily production of CSF alone. A pressure drop across the aqueduct of 0.62Pa is required to move a flow rate of 0.0058 mls^{-1} of CSF, which is equivalent to 5.78 mm^{3}s^{-1} of CSF. The findings also show that CSF velocities within the lateral ventricles of the HVS vary dramatically, with areas in the posterior horns of the ventricles seeing velocities of less than 10 nano ms^{-1}. These low velocities have various implications for cerebral drug delivery, as an injection of a drug is likely to stagnate in this area, rather than flow through the system.

References

Loth, F., Yardimci, M.A. and Alperin, N. (2001). Hydrodynamic modelling of cerebrospinal fluid motion within the spinal cavity. *Journal of Biomechanical Engineering*. 123(1): 71-9.

Zainy, M. (2002). Hydrodynamic modelling of cerebrospinal fluid motion within the human ventricular system. PhD thesis, University of Nottingham.

Greitz, D., Wirestam, R., Franck, A., Nordell, B., Thomsen, C. and Stahlberg, F. (1992). Pulsatile brain movement and associated hydrodynamics. *Diagnostic Neuroradiology*. 34(5): 370-380.

Greitz, D. (1993). Cerebrospinal fluid circulation and associated intracranial dynamics. A radiologic investigation using MR imaging and radionuclide cisternography. Acta Radiologica – Supplementum. (386): 1-23.

Aroussi, A., Zainy, M. and Vloeberghs M. (2000). Cerebrospinal fluid Dynamics In the Aqueduct of Sylvius. Proceedings of the 9th International Symposium on Flow Visualization. Edinburgh, Edinburgh University.

Howden, L., Aroussi, A., Vloeberghs, M., 2002, Drug Delivery to the Human Brain via the Cerebrospinal Fluid. Proceedings of the 11th Annual Conference of the CFD Society of Canada. Vancouver, University of British Columbia, 31 May-3 June.

Jacobson, E.E., Fletcher, D.F., Morgan, M.K. and Johnston, I.H. (1996). Fluid Dynamics of the Cerebral Aqueduct. Pediatric Neurosurgery. (24): 229-236.

Jacobson, E.E., Fletcher, D.F., Morgan, M.K. and Johnston, I.H. (1999). Computer modelling of the cerebrospinal fluid flow dynamics of aqueduct stenosis. Medical and biological engineering & computing. 37(1): 59-63.

Siegal, T. and Zylber-Katz, E. (2002), Strategies for increasing drug delivery to the brain. Clinical Pharmocokinetics. 41(3): 171-186

Redzic, Z.B., Segal, M.B. and (2004). The structure of the choroid plexus and the physiology of the choroid plexus epithelium. Advanced Drug Delivery Reviews. 56(12): 1695-716.

Perez-Figares, J.M., Jimenez, A.J. and Rodriguez, E.M. (2001). Subcommissural organ, cerebrospinal fluid circulation, and hydrocephalus. Microscopy Research & Technique. 52(5): 591-607.

Marieb, E.N. (2004) Human Anatomy & Physiology. Sixth Edition. Pearson Benjamin Cummings, San Francisco: 434.

Fin, L. and Grebe, R. (2003). Three dimensional modelling of the cerebrospinal fluid dynamics and brain interactions in the aqueduct of Sylvius. Computer Methods In Biomechanics and Biomedical Engineering. 6(3): 163-170.

H. Davson, K. Welch and M.B. Segal (1987). The Physiology and Pathophysiology of the Cerebrospinal Fluid. Churchill Livingstone Inc.: 751-755.

A. AROUSSI, School of Mechanical Engineering, University of Nottingham Malaysia Campus, Jalan Broga, Semenyih 43500 Selangor Darul Ehsan Malaysia. A.Aroussi@Nottingham.edu.my

L. HOWDEN, School of Mechanical, Material, Manufacturing Engineering and Managements, University of Nottingham, University Park, Nottingham, NG7 2RD, UK.

C. M. VLOEBERGHS, Queens Medical Centre, Department of Child Health, Nottingham NG7, UK